

Cell Type–Specific Chromatin Decondensation of a Metabolic Gene Cluster in Oats

Eva Wegel,^{a,1} Rachil Koumproglou,^b Peter Shaw,^b and Anne Osbourn^{a,2}

^aDepartment of Metabolic Biology, John Innes Centre, Norwich NR4 7UH, United Kingdom

^bDepartment of Cell and Developmental Biology, John Innes Centre, Norwich NR4 7UH, United Kingdom

Transcription-related chromatin decondensation has been studied in mammals for clusters of structurally and/or functionally related genes that are coordinately regulated (e.g., the homeobox locus in mice and the major histocompatibility complex locus in humans). Plant genes have generally been considered to be randomly distributed throughout the genome, although several examples of metabolic gene clusters for synthesis of plant defense compounds have recently been discovered. Clustering provides for genetic linkage of genes that together confer a selective advantage and may also facilitate coordinate regulation of gene expression by enabling localized changes in chromatin structure. Here, we use cytological methods to investigate components of a metabolic gene cluster for synthesis of developmentally regulated defense compounds (avenacins) in diploid oat (*Avena strigosa*). Our experiments reveal that expression of the avenacin gene cluster is associated with cell type–specific chromatin decondensation, providing new insights into regulation of gene clusters in plants. Importantly, chromatin decondensation could be visualized not only at the large-scale level but down to the single gene level. We further show that the avenacin and sterol pathways are likely to be inversely regulated at the level of transcription.

INTRODUCTION

In mammalian systems, transcription-related chromatin decondensation has been observed in a number of artificial gene clusters, in highly transcribed chromosomal regions and for clusters of functionally related genes that are coordinately regulated during development or between different cells types, such as the *Hoxb* locus (Tumbar et al., 1999; Tsukamoto et al., 2000; Volpi et al., 2000; Williams et al., 2002; Chambeyron and Bickmore, 2004; Janicki et al., 2004; Chambeyron et al., 2005; Sproul et al., 2005; Morey et al., 2007). In plants, genes are normally considered to be randomly distributed throughout the genome, with the obvious exception of groups of physically linked genes that share sequence homology and that have arisen through tandem gene duplication (e.g., gene-for-gene type disease resistance genes) (Friedman and Baker, 2007). Recently, however, several examples of clusters of genes for synthesis of plant defense compounds have been found (Frey et al., 1997; Qi et al., 2004; Wilderman et al., 2004; Shimura et al., 2007; Field and Osbourn, 2008; Swaminathan et al., 2009). The identification of groups of genes that do not share sequence relatedness and

that contribute to a common pathway raises some intriguing questions about the evolutionary pressures responsible for such self-organization (Amoutzias and Van de Peer, 2008). Clustering will facilitate the inheritance of beneficial combinations of genes that together confer a selective advantage (Gierl and Frey, 2001; Qi et al., 2004; Wong and Wolfe, 2005; Field and Osbourn, 2008), while disruption of such metabolic gene clusters may lead not only to loss of ability to synthesize a beneficial pathway end product but also to accumulation of toxic pathway intermediates (Field and Osbourn, 2008; Mylona et al., 2008). Physical clustering may also facilitate coordinate regulation of expression of pathway genes by enabling localized changes in chromatin structure (Sproul et al., 2005; Osbourn and Field, 2009).

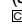
Our investigations of the role of natural products in plant defense have led us to identify an operon-like gene cluster for the synthesis of antimicrobial terpenes (avenacins) in diploid oat (*Avena strigosa*) (Papadopoulou et al., 1999; Qi et al., 2004). These defense compounds accumulate in the roots, where they confer broad-spectrum resistance to attack by soil-borne pathogens (Papadopoulou et al., 1999). The ability to produce avenacins is restricted to the genus *Avena* and has evolved since the divergence of oats from other cereals and grasses. To date, we have cloned a total of five genes in this cluster and have defined a further two loci that show complete genetic cosegregation with these five genes (Papadopoulou et al., 1999; Haralampidis et al., 2001; Qi et al., 2004, 2006; Mugford et al., 2009). The expression of the avenacin biosynthesis genes is tightly regulated and is restricted to the epidermal cells of the root meristem, which is the site of accumulation of avenacins (Haralampidis et al., 2001; Qi et al., 2006; Mugford et al., 2009).

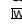
Here, we have selected the avenacin biosynthetic genes *Sad1* and *Sad2* for cytological investigation of chromatin

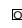
¹ Department of Genetics, University of Cambridge, Cambridge CB2 3EH, United Kingdom.

² Address correspondence to anne.osbourn@bbsrc.ac.uk.

The author responsible for distribution of materials integral to the findings presented in this article in accordance with the policy described in the Instructions for Authors (www.plantcell.org) is: Anne Osbourn (anne.osbourn@bbsrc.ac.uk).

 Some figures in this article are displayed in color online but in black and white in the print edition.

 Online version contains Web-only data.

 Open Access articles can be viewed online without a subscription.

www.plantcell.org/cgi/doi/10.1105/tpc.109.072124

decondensation in oat. *Sad1* and *Sad2* are adjacent genes that lie ~60 kb apart from each other. The two genes are separated by an intervening intergenic sequence that contains repetitive elements but no obvious open reading frames (Qi et al., 2006). *Sad1* encodes the enzyme that catalyzes the first committed step in the avenacin pathway (the oxidosqualene cyclase, β -amyrin synthase) (Haralampidis et al., 2001), and *Sad2* encodes a cytochrome P450 that is required for further modification of the product of SAD1 action, β -amyrin (Qi et al., 2006). *Sad1* and *Sad2* are particularly amenable for study because, in addition to encoding key early pathway enzymes, these genes are longer than the other genes in the cluster and so are particularly amenable to cytological analysis. Here, we use mRNA and DNA in situ hybridization, focusing on *Sad1* and *Sad2*, to investigate the relationship between cell type-specific gene expression and chromatin decondensation within the oat gene cluster.

RESULTS

Sad1 and *Sad2* Are Cotranscribed in Root Epidermis Cells and Are Transcriptionally Silent in the Cortex

Avenacin A-1 is the major UV fluorescent compound present in oat roots and accumulates in the epidermal cells of the root tips, which are the site of synthesis (Hostettmann and Marston, 1995; Haralampidis et al., 2001; Qi et al., 2006; Mugford et al., 2009) (Figures 1A and 1B). We used mRNA fluorescence in situ hybridization (FISH) to examine the expression of the *Sad1* and *Sad2* genes in root cells. All experiments were performed on wax-embedded root sections of 3-d-old seedlings of *A. strigosa*. *Sad1* and *Sad2* were simultaneously transcriptionally active in the nuclei of over 80% of root tip epidermal cells (Figure 1C, Table 1). Sense probes for these genes did not give signals, indicating that the signals that we observed were derived from mRNA and not DNA (see Supplemental Figure 1 online). *Sad1* was additionally expressed in ~50% of the cells of the outermost cortex layer, referred to here as the subepidermis (Figures 1A and 1C), while *Sad2* transcripts were seldom detected in this cell layer. *Sad1* and *Sad2* transcripts were not observed in other cell types within the root (see Supplemental Figure 1 online). There were no obvious differences between G1 and G2 nuclei in coexpression of *Sad1* and *Sad2* in root tip epidermal cells (Figure 1C), implying that expression of *Sad1* and *Sad2* is not cell cycle dependent.

Cytoplasmic proteins and nuclear-encoded plastid and mitochondrial proteins are generally translated on free ribosomes in the cytoplasm, while integral membrane proteins and those that are secreted are translated on ribosomes bound to the ER. SAD1 and SAD2 are not predicted to be integral membrane proteins, but based on structural predictions and by analogy with their sterol biosynthetic counterparts, both are likely to be membrane associated (Haralampidis et al., 2001; Qi et al., 2004, 2006). In addition to the nascent transcripts that we detected in the nuclei (Figure 1), cytoplasmic transcripts derived from *Sad1* and *Sad2* were readily detectable in the root tip epidermal cells (Figure 2). Cytoplasmic *Sad1* transcript was also evident at lower levels in the cytoplasm of the cells of the subepidermis (see Supplemental

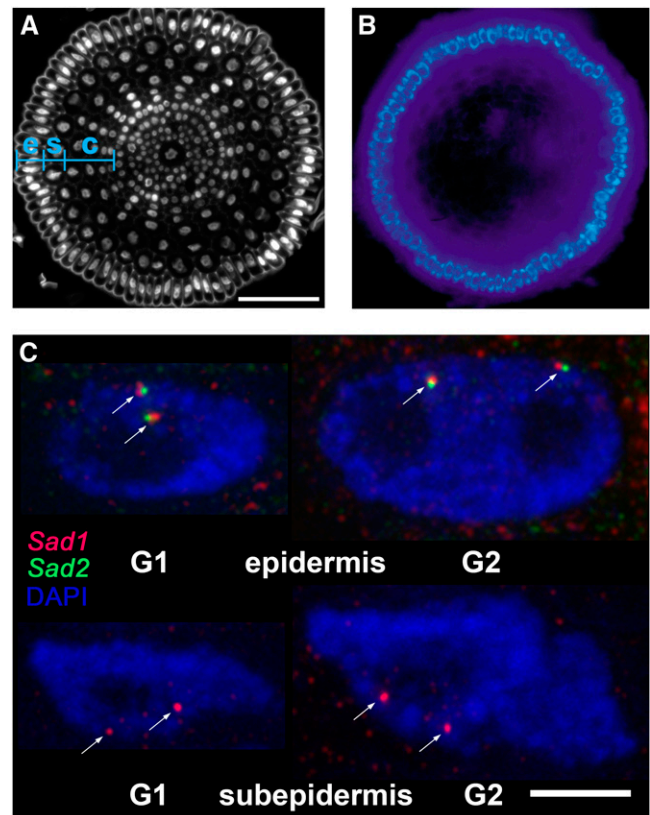


Figure 1. Visualization of Nascent *Sad1* and *Sad2* Transcripts in Nuclei of Oat Root Tip Cells.

(A) Cross section of an oat root tip with nuclei stained with 4',6-diamidino-2-phenylindole (DAPI) showing the different cell types (e, epidermis; s, subepidermis; c, cortex). Bar = 50 μ m.
(B) Fluorescence of avenacin A-1 in the root tip epidermal cells.
(C) Detection of *Sad1* (red) and *Sad2* (green) transcripts in nuclei of root tip cells; blue, chromatin stained with DAPI. Representative G1 and G2 nuclei are shown for the epidermal and subepidermal calls. The images are overlays of 27 optical sections with section spacing of 0.2 μ m. Arrows indicate the nuclear sites of nascent transcripts. In each panel of **(C)**, a single nucleus is shown. Bar = 5 μ m.

Figure 2 online). The spatial pattern of the *Sad2* transcript resembled a typical reticulate endoplasmic reticulum (ER) distribution in the cytoplasm. By contrast, the *Sad1* transcript was localized in foci that may represent branched strands of a membranous system, possibly specialized subdomains of the ER. These experiments indicate that the patterns of localization of the *Sad1* and *Sad2* mRNAs in the cytoplasm are distinct and rarely overlap, suggesting that the translation of these two mRNA species into proteins is unlikely to be spatially coordinated. A few examples of targeting of transcripts to specific parts of the cytoplasm in plant cells have been reported, including transcripts for expansins and seed storage proteins (Choi et al., 2000; Okita and Choi, 2002; Crofts et al., 2004; Washida et al., 2004). Avenacins accumulate in the cell vacuole (Mylona et al., 2008), but the route by which pathway intermediates are transported from the ER to this final destination is

Table 1. Detection of Nascent Transcripts of *Sad1* and *Sad2* in the Nuclei of Cells within the Oat Root Tip

Cell Type	Percentage of Alleles Expressing:				Total
	<i>Sad1</i> + <i>Sad2</i>	<i>Sad1</i>	<i>Sad2</i>	Neither	
Epidermis	81.4	1.8	9.5	7.3	100
Subepidermis	2.1	50.7	0.7	46.4	100

Total alleles counted: Epidermis, 220; subepidermis, 140.

unknown. It is possible that this process could be mediated via zip-coded regions of the ER (Grotewold and Davies, 2008).

The Genomic Region Spanning *Sad1* and *Sad2* Is Decondensed in the Root Epidermis

We then used DNA FISH to determine whether expression of genes within the avenacin gene cluster is accompanied by chromatin decondensation. Previously, we constructed and sequenced a BAC contig spanning the *Sad1/Sad2* region and showed that these two genes lie within 58 kb of each other in the *A. strigosa* genome (Figure 3A) (Qi et al., 2004, 2006). We generated probes for the *Sad1* and *Sad2* genes (15.2 and 5.8 kb, respectively) (Figure 3A). Using these probes, we were able to detect the *Sad1* and *Sad2* loci in nuclei of the epidermal, subepidermal, and cortical cells of *A. strigosa* root tips by DNA FISH (Figures 3B and 3C). The hybridization signal for *Sad1* in the nuclei of epidermal cells frequently comprised more than one fluorescent focus. In several cases, this was also true for *Sad2*. However, in the subepidermal and cortical cells, each locus was almost always visualized as a discrete focus. The nuclei that we examined in these experiments were all G1 nuclei (see Methods) and so these multiple foci are not attributable to signals derived from sister chromatids. The multiple foci that we have observed for *Sad1* (and to a lesser extent *Sad2*) in the nuclei of the root tip epidermal cells are therefore likely to reflect decondensation of the respective loci. Beaded signals have also been seen in much larger, transcriptionally active chromosome regions spanning groups of major histocompatibility complex and other genes in mammalian cells (Volpi et al., 2000; Müller et al., 2004).

We then examined the length of the region encompassing *Sad1* and *Sad2* in the nuclei of the epidermal, subepidermal, and cortical cells. To do this, we measured a path consisting of the shortest distance in three dimensions traversing the intensity maxima of all fluorescent foci, starting with all *Sad1* foci (green) and ending with all *Sad2* foci (red), as shown by Figure 3C and the accompanying path outlines (Figure 3D). These data are summarized in Figure 3E. We calculated a mean length for the whole region of 0.97 μm for epidermis nuclei and of 0.41 and 0.42 μm for subepidermis and cortex nuclei, respectively. The length differences between epidermis and subepidermis/cortex are significant ($P = 0.0001$ for both, two-tailed Mann-Whitney U-test) and correspond to a chromatin compaction of 28-fold for the epidermis and 66- and 65-fold for subepidermis and cortical cells, compared with naked B-DNA (Watson and Crick, 1953). The length differences between subepidermal and cortical cells are not significant ($P = 0.7$, two-tailed Mann-Whitney U-test). Thus, the region shown

in Figure 3A is more extended in nuclei of cells expressing both *Sad1* and *Sad2* (the epidermal cells) than in those cells that do not express these genes (the cortical cells) or in the subepidermal cell layer where *Sad1* is expressed more sporadically and at lower levels. This suggests that coordinate expression of *Sad1* and *Sad2* in the root epidermal cells may be associated with chromatin decondensation. However, lower-level expression of *Sad1* in the subepidermal cell layer is not associated with significant chromatin decondensation as assessed using these methods. In order to distinguish the contributions of the two genes to chromatin decondensation from that made by the intergenic sequence, we compared the distances between the closest *Sad1* and *Sad2* foci for each chromosome that we examined, as an estimated lower bound for the intergenic distance. The mean lengths obtained were 0.47 μm for epidermis nuclei and 0.31 and 0.34 μm for subepidermal and cortex nuclei, respectively. These differences between epidermis and subepidermis/cortex nuclei were significant ($P = 0.03$ for the difference between epidermis and cortex and $P = 0.02$ for the difference between epidermis and subepidermis, two-tailed Mann-Whitney U-test). There was no significant difference in the length of the intergenic regions when the values for subepidermis and cortex were compared ($P = 0.9$, two-tailed Mann-Whitney U-test). Our strategy for defining the paths that we have measured is based on the assumption that the closest foci that we observe for each gene are nearest neighbors in terms of the linear organization of the gene and that the *Sad1* and *Sad2* foci that are closest to each other represent the shortest intergenic distance. Clearly, this need not always be the case, and so we may have underestimated the degree of chromatin decondensation for both of these parameters.

Sad1 Is Decondensed in the Root Epidermis

Next, we examined decondensation at the single gene level. First, we performed DNA FISH experiments using the

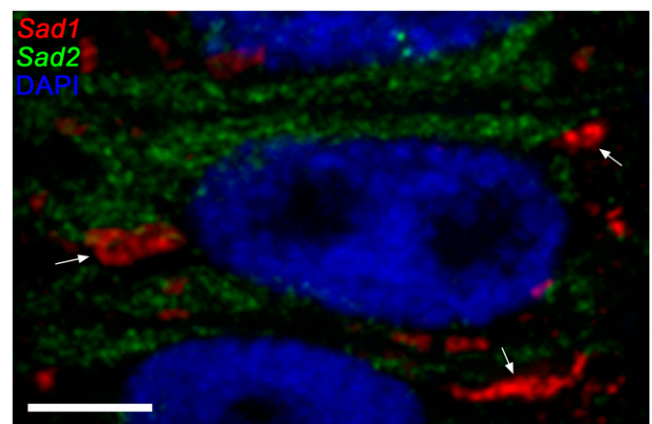


Figure 2. Localization of Cytoplasmic Transcripts Derived from *Sad1* and *Sad2*.

Cytoplasmic localization of *Sad1* and *Sad2* transcripts in oat root epidermal cells visualized by mRNA FISH. The *Sad1* transcript (red) is localized in discrete foci (examples shown by the arrows), while the *Sad2* transcript (green) shows a reticulate distribution suggestive of localization to the reticulate ER. Blue, chromatin stained with DAPI. Bar = 5 μm .

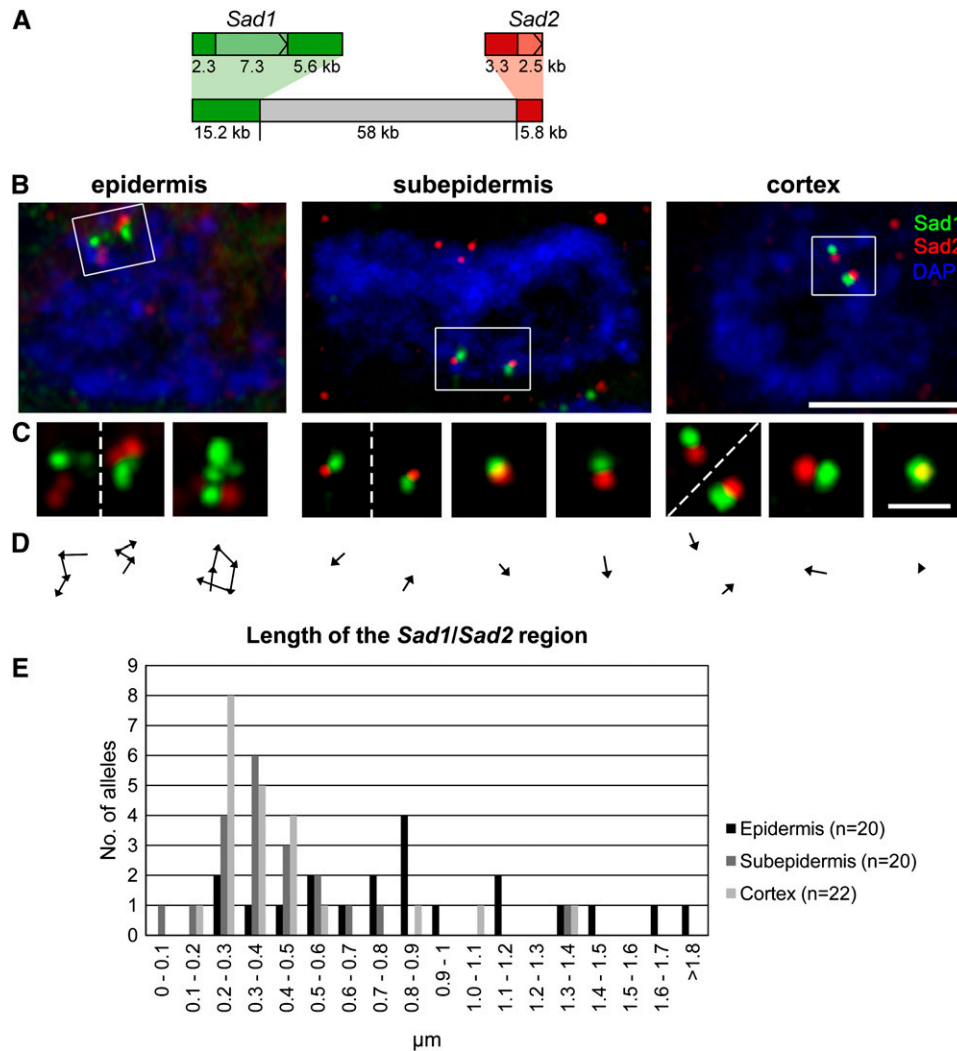


Figure 3. Chromatin Decondensation in the *Sad1/Sad2* Region.

(A) Diagram showing the *Sad1* (green) and *Sad2* (red) probes used for DNA in situ hybridization (coding regions in lighter shades of green and red). (B) The *Sad1/Sad2* region is decondensed in the nuclei of epidermal cells (left) compared with those of the subepidermis (center) and the cortex (right). In each panel, a single nucleus is shown. Bar = 5 μ m. (C) Detailed views of individual gene regions. Dashed lines separate loci on two adjacent chromosomes. Bar = 1 μ m. The images shown in (B) and (C) are overlays of several optical sections, section spacing 0.2 μ m. Blue, chromatin stained with DAPI. (D) Line drawings showing the minimum paths measured in (C), starting from *Sad1*. (E) Length distributions of the *Sad1/Sad2* region in nuclei of epidermal, subepidermal, and cortical cells.

same 15.2-kb *Sad1* probe as in our previous experiments (Figures 3A and 4A) and analyzed the number of fluorescent foci in G1 and G2 nuclei of cells in the epidermis, subepidermis, and cortex of the root tips (Figures 4B and 4C) by three-dimensional optical sectioning through the nuclei. There were more fluorescent foci for *Sad1* in the nuclei of epidermal cells when compared with the nuclei of subepidermal and cortical cells, consistent with decondensation of *Sad1* in the nuclei of the epidermal cells. These differences were significant for both G1 and G2 nuclei (G1, $P = 0.001$; G2, $P = 0.002$, for epidermis compared with subepidermis; G1, $P = 0.000004$; G2, $P = 0.00002$ for epidermis compared with cortex; Figure 4C). There also appeared to be

more *Sad1* foci in the subepidermis compared with the cortex, although these differences were significant for G2 nuclei ($P = 0.03$) but not for G1 nuclei ($P = 0.2$). These results are consistent with our expression data (Figure 1C, Table 1), which indicate that *Sad1* is expressed in the nuclei of root epidermal cells and to a lesser extent in nuclei of the subepidermal cells but not in the cortex. *Sad1* shows an intermediate degree of decondensation when G2 nuclei of the cortex, subepidermis, and epidermis are compared (Figure 4), although cell cycle-related differences in *Sad1* expression were not observed (Figure 1).

We then labeled the 5' and 3' parts of the *Sad1* locus with different fluorochromes (Figure 5). In this case, we did not

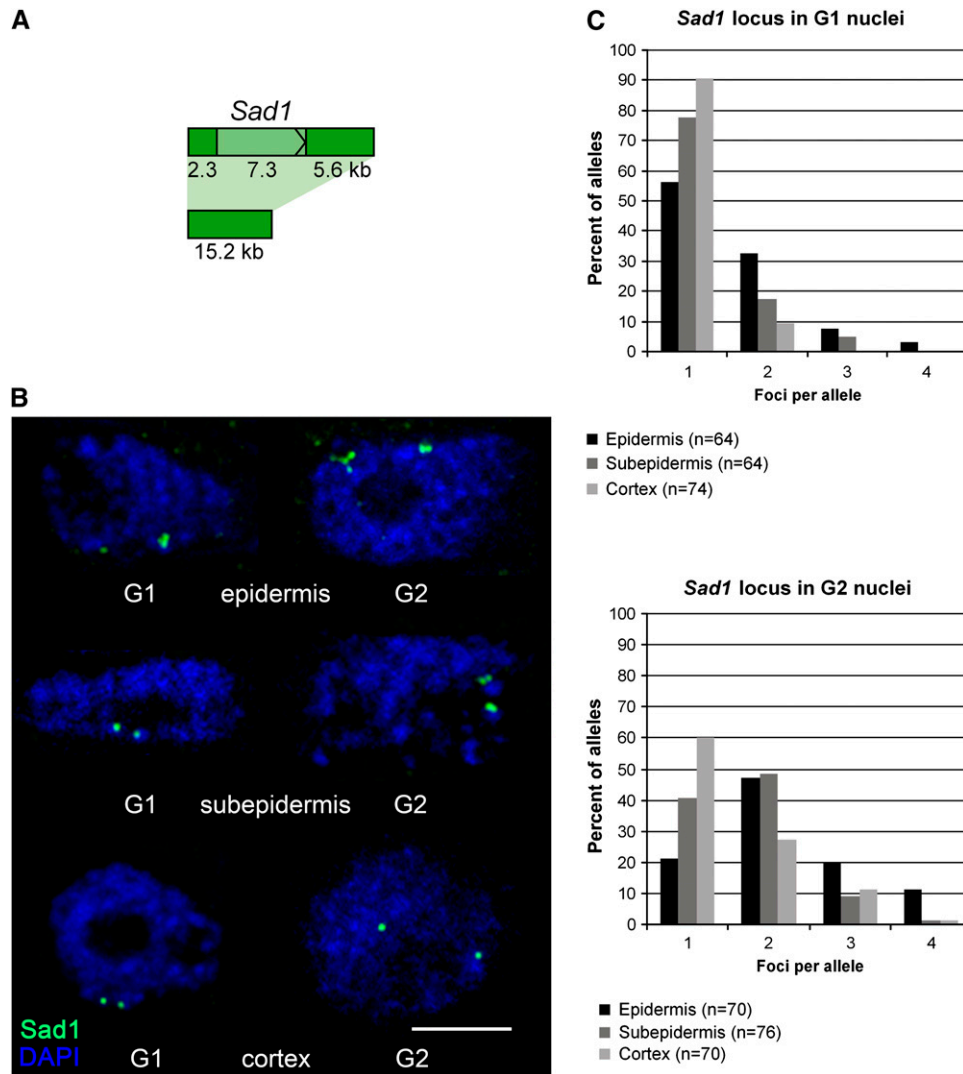


Figure 4. The *Sad1* Gene Locus Is Decondensed in Nuclei of Root Tip Epidermal Cells as Shown Using a 15.2-kb Probe Spanning *Sad1*.

(A) Diagram showing the 15.2-kb probe spanning the *Sad1* gene locus used for DNA in situ hybridization (coding region in light green).

(B) Representative examples of *Sad1* loci in different cell types. The images are overlays of several optical sections, section spacing 0.2 μm . Blue, chromatin stained with DAPI. Bar = 5 μm .

(C) Distributions of numbers of fluorescent foci in G1 and G2 nuclei in the three different cell types.

differentiate between G1 and G2 nuclei. We restricted our analysis to those loci that showed one green and one red focus (and so represented either G1 nuclei or overlapping chromatids in G2 nuclei) or that showed two red and two green foci that could be identified as belonging to two different chromatids (Figures 5B and 5C). We then measured the distances in three dimensions between the intensity maxima of the two halves for nuclei of root epidermal and cortical cells (Figure 5D). Based on these measurements, the mean length of *Sad1* was calculated to be 0.35 μm in the epidermis and 0.23 μm in the cortex. This corresponds to a chromatin compaction of 15-fold in the epidermis and 22-fold in the cortex compared with naked B-DNA (Watson and Crick, 1953). These length differences are highly significant ($P = 0.0004$).

***CS1*, the *Sad1* Homolog in Sterol Biosynthesis, Is Expressed in the Root Cortex but Not in the Epidermis of the Root Tip**

Sad1 is likely to have been recruited from primary sterol metabolism by duplication of the cycloartenol synthase gene *CS1*, followed by acquisition of new function (Haralampidis et al., 2001; Qi et al., 2004). Sterols are essential for plant growth and development, and the genes for sterol biosynthesis are normally expressed throughout the plant (Ohya et al., 2009). Previously, we cloned and characterized the *A. strigosa CS1* gene and showed by RNA gel blot analysis that this gene (which shares 42% nucleotide sequence identity with *Sad1*) is expressed in the roots, stems, leaves, and flowers, as expected (Haralampidis

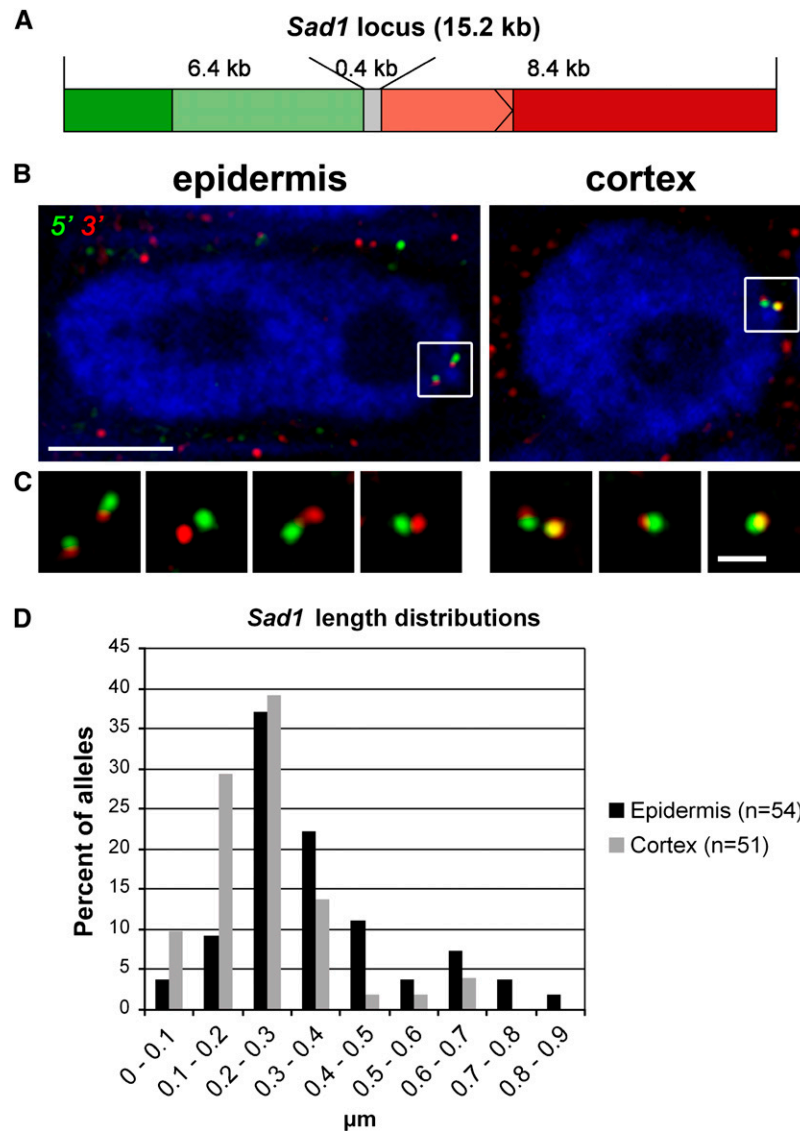


Figure 5. Decondensation of the *Sad1* Gene Locus Can Be Visualized Using Probes for the 5' and 3' Ends of the Gene.

(A) Diagram showing the probes for the 5' and 3' ends of the *Sad1* gene used for DNA in situ hybridization. The two probes split the locus in half. The parts of the coding region encompassed by each probe are shown in lighter shades of green or red.

(B) G2 nuclei in epidermal and cortical root cells each showing two *Sad1* loci: 5' probe in green and 3' probe in red. Bar = 5 μm .

(C) Detailed views of individual gene loci (with the framed loci shown in **[B]**) on the left of each set of panels. Bar = 1 μm . The images shown in **(B)** and **(C)** are overlays of several optical sections, section spacing 0.2 μm . Blue, chromatin stained with DAPI.

(D) Length distributions of the *Sad1* locus in nuclei of epidermal and cortical cells. The length of each locus was determined by measuring the distance in three dimensions between the intensity maxima of the two halves.

et al., 2001; Qi et al., 2004). Here, we have performed mRNA in situ hybridization using alkaline phosphatase signal amplification to examine the spatial expression pattern of *CS1* at higher resolution. Surprisingly, we found that *CS1* transcripts were not detectable in the root tip. While *Sad1* transcripts were detected primarily in the epidermal cells of the meristematic zone of the root tips of 3-d-old *A. strigosa* seedlings (and more weakly in the subepidermal cell layer and in parts of the columella), *CS1* transcripts were only evident in the cortical cells behind this

region (Figure 6). This suggests that the two pathways are likely to be inversely regulated at the level of transcription. Inverse coordinate regulation of the two pathways may be important because the two pathways compete for a common substrate (2,3-oxidosqualene) (Chappell, 2002). It could also represent a self-protection mechanism, since amphipathic triterpene glycosides, such as avenacins, exert their toxic effects on cells by complexing with sterols, causing membrane permeabilization (Morrissey and Osbourn, 1999). A cycloartenol

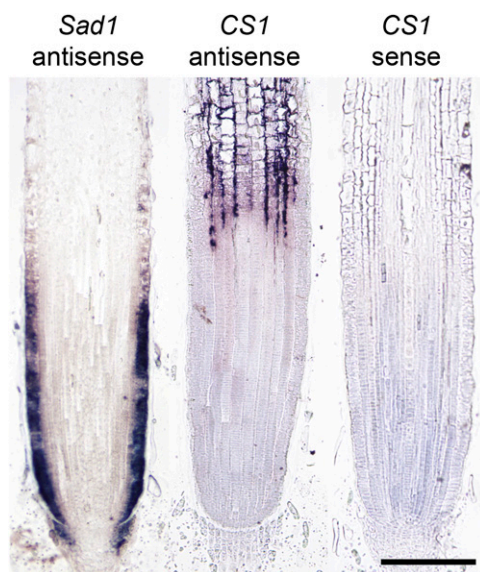


Figure 6. Distributions of *Sad1* and Cycloartenol Synthase Transcripts in the Root Tip.

In situ mRNA hybridization of young root tips. *Sad1* is expressed in the epidermis and weakly in parts of the subepidermis of the root tip and some columella cells, and *CS1* expression is restricted to the cortex and starts in the elongation zone above the root tip. Bar = 200 μm .

[See online article for color version of this figure.]

synthase-independent pathway to plant sterols that involves synthesis of low levels of sterols via lanosterol has recently been described (Ohya et al., 2009). It is possible that the cells of the root meristem synthesize essential sterols via this route.

The coding regions (including introns) of *Sad1* and *CS1* are of similar length (7.3 and 7.6 kb, respectively). *CS1* is not expressed at detectable levels in the root meristem and is unlinked to *Sad1* (Qi et al., 2004). We labeled 10.5-kb sequences comprising the coding regions and 3' flanks for each of the two genes (Figure 7A) and used these in DNA FISH experiments to compare the behavior of the *Sad1* and *CS1* loci in the nuclei of epidermal and cortical cells within the root tip (Figure 7B). We selected G2 nuclei for these experiments because the hybridization signals are more readily visible. Analysis of the number of fluorescent foci that were detected for the two loci in the nuclei of epidermal and cortical cells revealed that *Sad1* is significantly more decondensed than *CS1* in epidermal cells ($P = 0.01$). This confirms our previous findings that expression of *Sad1* in the nuclei of epidermal cells is associated with chromatin decondensation at the *Sad1* locus. By contrast, both the *Sad1* and *CS1* loci are condensed in the nuclei of cortical cells, and there is no significant difference in the number of foci observed for each ($P = 0.6$). Equally, there is no significant difference in the number of foci observed for *CS1* loci in the nuclei of cortical and epidermal cells ($P = 0.2$). These experiments indicate that the differences in the degree of chromatin decondensation of the *Sad1* locus in the epidermal and cortical cells of the root are unlikely to be due to general differences in chromatin conformation or compaction between the two cell types.

DISCUSSION

Previously, we showed that a multicopy transgene cluster in wheat (*Triticum aestivum*) containing endogenous genes for seed storage proteins under the control of their own promoters undergoes large-scale chromatin decondensation upon transcriptional activation during seed development (Wegel et al., 2005). Here, we have shown that a naturally occurring gene cluster for synthesis of developmentally regulated plant defense compounds decondenses in nuclei of root epidermal cells as assessed by cytological analysis of the region of the genome encompassing *Sad1* and *Sad2*. *Sad1* and *Sad2* are the longest genes in the cluster that we have so far identified, and this enabled us to image them, while the sequences of the other genes were below the detection limit. We were able to correlate the expression of *Sad1* and *Sad2* with an increase in both the number of foci of in situ labeling and with the minimum path length necessary to join the respective foci of the genes. The latter provides a minimum estimate for decondensation of the cluster and corresponds to 28- and 65-fold compaction compared with B-DNA for the epidermal and cortical cells, respectively. This is likely to be an underestimate since the actual length may be longer than the shortest path and also because the signal for the most decondensed regions may be too faint to be detected. In other systems, the appearance of multiple foci instead of continuous signal has been attributed to the underlying chromatin structure, with less densely packed (invisible) regions linking more densely packed (visible) regions (Volpi et al., 2000; Müller et al., 2004). The murine *HoxB* gene cluster has been shown to decondense from a DNA compaction of around 300- to ~ 34 -fold after activation (Chambeyron and Bickmore, 2004), while a 375-kb region of the human major histocompatibility complex (MHCII) has a DNA compaction of ~ 100 -fold before induction with interferon and ~ 60 -fold after induction (Müller et al., 2004; Table 2). In both these cases, the values are averaged over the whole region, and the compaction of the actual transcribed genes compared with the intergenic regions cannot be deduced. Our experiments suggest that the *Sad1* gene itself decondenses on activation, with a 15-fold compaction in the epidermis compared with 22-fold compaction in the cortex. This assumes a linear gene organization. If the active gene adopts a more complex structure, the compaction values are likely to be lower. The condensation state of the *Sad1* gene also seems to depend on its level of activity. Judging by the number of fluorescent foci, *Sad1* was more condensed in the subepidermis than in the epidermis. This is likely to be due to a combination of condensed, nonexpressing loci and also loci that are expressing at a lower level than in the epidermis. Transcriptional activity can precede any visible loosening of the chromatin structure (Janicki et al., 2004; Wegel et al., 2005), but as more genes within a colinear region decondense at the same time, the region itself becomes more decondensed, and this is likely to further facilitate expression. The fact that the intergenic region is only visibly decondensed in the nuclei of epidermal cells is consistent with this scenario.

The higher-order structure of chromatin is still a matter of considerable debate. There is good evidence that nucleosomes are organized into 10-nm fibers, visualized as beads on a string

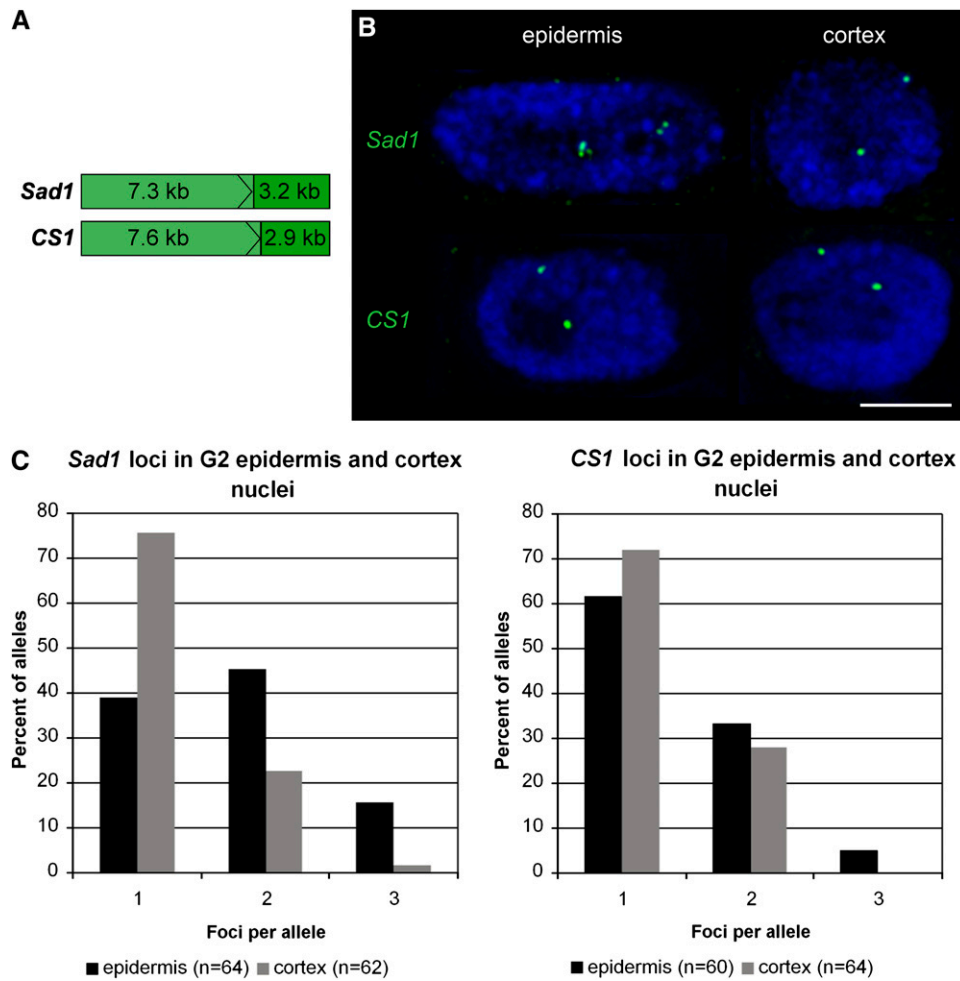


Figure 7. *Sad1* and *CS1* Loci in Epidermis and Cortex Nuclei.

(A) After in situ hybridization with 10.5-kb probes spanning the coding regions and 3' flanks of *Sad1* or *CS1*, the number of fluorescent foci per allele was determined in G2 root epidermis and cortex nuclei.

(B) Representative epidermis and cortex nuclei with *Sad1* or *CS1* labeling. Overlay of several optical sections; section spacing, 0.15 μm . Blue, chromatin stained with DAPI. Bar = 5 μm .

(C) Distributions of fluorescent foci in epidermis and cortex nuclei (*Sad1* appears more condensed in both the epidermis and the cortex than in Fig. 4 due to differences in probe lengths).

under the electron microscope, which would have a compaction of sevenfold (Table 2) (Olins and Olins, 1974; Oudet et al., 1975; Goodrich and Tweedie, 2002). Thus, our data for *Sad1* suggest that on average this gene is more compact than a 10-nm fiber, although it is likely that decondensation varies along the gene and may be greater where the polymerases are bound. There is very little data so far available about the condensation status of active genes. The Balbiani rings (giant chromosomal puffs) of the Dipteran midge *Chironomus* have been shown by electron microscopy to have a compaction of 3.6, well below that of the 10-nm fiber (Daneholt et al., 1982), while the rRNA genes in pea (*Pisum sativum*) show a greater degree of compaction (8- to 11-fold), which corresponds well with that of the 10-nm fiber (Gonzalez-Melendi et al., 2001) (Table 2). The *Chironomus* and pea genes studied in these investigations are very highly transcribed and

have many polymerases attached, which may be expected to lead to a higher degree of decondensation. Most active genes are likely to have only one or two polymerases attached, so our value of 15 for compaction of active *Sad1* seems reasonable.

The proposed levels of structural organization above the 10-nm fiber are highly controversial. A well-publicized secondary structure of chromatin is the 30-nm fiber, which is 40- to 50-fold more condensed than naked B-DNA (Goodrich and Tweedie, 2002). Such 30-nm fibers have been observed in vitro (Robinson et al., 2006), but as yet there is no clear evidence for these in vivo or, indeed, for more condensed higher-order structures (Branco and Pombo, 2007; Fakan and van Driel, 2007). Our mean chromatin compaction values indicate that in both the epidermis and the cortex, *Sad1* is packaged into a structure that has a higher packing order than the 10-nm fiber and a lower one than

Table 2. DNA Compaction

DNA	Size (kb)	Untranscribed Length		Compaction	Reference
		Transcribed Length (μm)	kb/ μm		
B-DNA	–	–	2.9	1.0	Watson and Crick (1953)
10-nm fiber	–	–	20.3	7.0	Woodcock and Dimitrov (2001)
30-nm fiber	–	–	116–145	40–50	Woodcock and Dimitrov (2001)
Hox1b-Hox9	90	0.1	900	310	Chambeyron and Bickmore (2004)
		0.9	100	34	
MHCII	375	1.2	312	107	Müller et al. (2004)
		2.1	178	61	
<i>Sad1-Sad2</i>	79	0.42 (cortex)	178	65	This study
		0.97 (epidermis)	81	28	
<i>Sad1</i>	15	0.23 (cortex)	65	22	This study
		0.35 (epidermis)	43	15	
Pea rDNA (transcribed)	6.6	0.2–0.3	22–33	7.6–11.4	Gonzalez-Melendi et al. (2001)
<i>Chironomus</i> BR2 (transcribed)	37	3.5	10.4	3.6	Daneholt et al. (1982)
Wheat glutenin array (20 copies)	180	2.17	83	29	Wegel et al. (2005)
		13.66	13	4.5	

the 30-nm fiber. For the *Sad1/Sad2* region with its repeat-rich intergenic region (Qi et al., 2006), the packing order increases but is still less than the 30-nm fiber level in the epidermis, while it is above this level in the cortex (Table 2).

Our data provide cytological evidence to link cell type-specific chromatin decondensation with expression of the avenacin gene cluster in nuclei of oat root epidermal cells, providing new insights into regulation of gene clusters in plants. It has been suggested that opening up domains of secondary chromatin structure may place genes in a transcriptionally permissive environment, where their expression can then be triggered by transcription factors (Sproul et al., 2005). Further experiments are required to establish the cause and effect of this phenomenon and to identify the factors required for pathway regulation. The most satisfactory way to achieve this will be through characterization of regulatory mutants. We have isolated a resource of ~100 avenacin-deficient mutants of *A. strigosa* (Papadopoulou et al., 1999; Qi et al., 2006; Mugford et al., 2009). Analysis of this mutant collection is expected to lead to the identification of loci that are required for regulation of expression of the gene cluster. These may include genes for pathway-specific transcription factors and also for regulation at the chromatin level.

METHODS

Plant Material

The diploid oat (*Avena strigosa*) accession number S75 (from the Institute of Grasslands and Environmental Research, Aberystwyth, Wales, UK) was used for all experiments.

RNA and DNA in Situ Hybridization

Oat seeds were imbibed in water for 24 h at 4°C and germinated on wet filter paper for 3 d at 22°C. Root tips were fixed in 4% (w/v) formaldehyde in PBS and embedded in wax and longitudinal sections (12 μm) prepared. Probes for in situ hybridization were prepared by in vitro transcription (for RNA probes) or by nick translation (for DNA probes) and labeled with either digoxigenin-11-UTP (Roche) or dinitrophenol-11-UTP (Perkin-

Elmer) (see Supplemental Methods online for further details of probes, hybridization, and immunodetection methods).

Image Acquisition, Analysis, and Measurements

RNA in situ experiments with enzymatic detection were analyzed with a Nikon Eclipse 800 microscope using a $\times 10$ objective with a numerical aperture of 0.3. Images were taken on a Pixera Pro 600 digital camera. For the FISH experiment, root sections were analyzed using a $\times 60$ objective (numerical aperture 1.4, oil) on a Nikon Eclipse 600 microscope equipped with a Hamamatsu Orca ER cooled CCD digital camera, a motorized xy stage, and a z-focus drive. Further details concerning filters, correction of chromatic aberration, deconvolution of raw data, differentiation between G1 and G2 nuclei, length measurements, and preparation of images are given in Supplemental Methods online.

Accession Numbers

Sequence data for the genes referred to in this article can be found in the GenBank/EMBL data libraries under accession numbers DQ680849 (*Sad1* and *Sad2*) and AY618693 (*CS1*).

Supplemental Data

The following materials are available in the online version of this article:

Supplemental Figure 1. Control RNA in Situ Hybridization Experiments for *Sad1* and *Sad2*.

Supplemental Figure 2. Transcripts of *Sad1* (red) and *Sad2* (green) in Oat Root Tips.

Supplemental Methods.

ACKNOWLEDGMENT

This project was funded by the Biotechnology and Biological Sciences Research Council, UK (Grant BB/C504435/1).

Received October 12, 2009; revised November 29, 2009; accepted December 4, 2009; published December 29, 2009.

REFERENCES

- Amoutzias, G., and Van de Peer, Y.** (2008). Together we stand: Genes cluster to coordinate regulation. *Dev. Cell* **14**: 640–642.
- Branco, M.R., and Pombo, A.** (2007). Chromosome organization: New facts, new models. *Trends Cell Biol.* **17**: 127–134.
- Chambeyron, S., and Bickmore, W.A.** (2004). Chromatin decondensation and nuclear reorganization of the HoxB locus upon induction of transcription. *Genes Dev.* **18**: 1119–1130.
- Chambeyron, S., Da Silva, N.R., Lawson, K.A., and Bickmore, W.A.** (2005). Nuclear re-organisation of the Hoxb complex during mouse embryonic development. *Development* **132**: 2215–2223.
- Chappell, J.** (2002). The genetics and molecular genetics of terpene and sterol origami. *Curr. Opin. Plant Biol.* **5**: 151–157.
- Choi, S.B., Wang, C., Muench, D.G., Ozawa, K., Franceschi, V.R., Wu, Y., and Okita, T.W.** (2000). Messenger RNA targeting of rice seed storage proteins to specific ER subdomains. *Nature* **407**: 765–767.
- Crofts, A.J., Washida, H., Okita, T.W., Ogawa, M., Kumamaru, T., and Satoh, H.** (2004). Targeting of proteins to endoplasmic reticulum-derived compartments in plants. The importance of RNA localization. *Plant Physiol.* **136**: 3414–3419.
- Daneholt, B., Andersson, K., Bjorkroth, B., and Lamb, M.M.** (1982). Visualization of active 75 S RNA genes in the Balbiani rings of *Chironomus tentans*. *Eur. J. Cell Biol.* **26**: 325–332.
- Fakan, S., and van Driel, R.** (2007). The perichromatin region: A functional compartment in the nucleus that determines large-scale chromatin folding. *Semin. Cell Dev. Biol.* **18**: 676–681.
- Field, B., and Osbourn, A.E.** (2008). Metabolic diversification - Independent assembly of operon-like gene clusters in different plants. *Science* **320**: 543–547.
- Frey, M., Chomet, P., Glawischnig, E., Stettner, C., Grun, S., Winklmaier, A., Eisenreich, W., Bacher, A., Meeley, R.B., Briggs, S.P., Simcox, K., and Gierl, A.** (1997). Analysis of a chemical plant defense mechanism in grasses. *Science* **277**: 696–699.
- Friedman, A.R., and Baker, B.J.** (2007). The evolution of resistance genes in multi-protein plant resistance systems. *Curr. Opin. Genet. Dev.* **17**: 493–499.
- Gierl, A., and Frey, M.** (2001). Evolution of benzoxazinone biosynthesis and indole production in maize. *Planta* **213**: 493–498.
- Gonzalez-Melendi, P., Wells, B., Beven, A.F., and Shaw, P.J.** (2001). Single ribosomal transcription units are linear, compacted Christmas trees in plant nucleoli. *Plant J.* **27**: 223–233.
- Goodrich, J., and Tweedie, S.** (2002). Remembrance of things past: Chromatin remodeling in plant development. *Annu. Rev. Cell Dev. Biol.* **18**: 707–746.
- Grotewold, E., and Davies, K.** (2008). Trafficking and sequestration of anthocyanins. *Nat. Prod. Comms.* **3**: 1251–1258.
- Haralampidis, K., Bryan, G., Qi, X., Papadopoulou, K., Bakht, S., Melton, R., and Osbourn, A.** (2001). A new class of oxidosqualene cyclases directs synthesis of antimicrobial phytoprotectants in monocots. *Proc. Natl. Acad. Sci. USA* **98**: 13431–13436.
- Hostettmann, K., and Marston, A.** (1995). *Chemistry and Pharmacology of Natural Products: Saponins*. (Cambridge, UK: Cambridge University Press).
- Janicki, S.M., Tsukamoto, T., Salghetti, S.E., Tansey, W.P., Sachidanandam, R., Prasanth, K.V., Ried, T., Shav-Tal, Y., Bertrand, E., Singer, R.H., and Spector, D.L.** (2004). From silencing to gene expression: Real-time analysis in single cells. *Cell* **116**: 683–698.
- Morey, C., Da Silva, N.R., Perry, P., and Bickmore, W.A.** (2007). Nuclear reorganisation and chromatin decondensation are conserved, but distinct, mechanisms linked to Hox gene activation. *Development* **134**: 909–919.
- Morrissey, J.P., and Osbourn, A.E.** (1999). Fungal resistance to plant antibiotics as a mechanism of pathogenesis. *Microbiol. Mol. Biol. Rev.* **63**: 708–724.
- Mugford, S.T., et al.** (2009). A serine carboxypeptidase-like acyltransferase is required for synthesis of antimicrobial compounds and disease resistance in oats. *Plant Cell* **21**: 2473–2484.
- Müller, W.G., Rieder, D., Kreth, G., Cremer, C., Trajanoski, Z., and McNally, J.G.** (2004). Generic features of tertiary chromatin structure as detected in natural chromosomes. *Mol. Cell. Biol.* **24**: 9359–9370.
- Mylona, P., Owatworakit, A., Papadopoulou, K., Jenner, H., Qin, B., Findlay, K., Hill, L., Qi, X., Bakht, S., Melton, R., and Osbourn, A.** (2008). *Sad3* and *Sad4* are required for saponin biosynthesis and root development in oat. *Plant Cell* **20**: 201–212.
- Ohyama, K., Suzuki, M., Kikuchi, J., Saito, K., and Muranaka, T.** (2009). Dual biosynthetic pathways to phytosterol via cycloartenol and lanosterol in *Arabidopsis*. *Proc. Natl. Acad. Sci. USA* **106**: 725–730.
- Okita, T.W., and Choi, S.B.** (2002). mRNA localization in plants: Targeting to the cell's cortical region and beyond. *Curr. Opin. Plant Biol.* **5**: 553–559.
- Olins, A.L., and Olins, D.E.** (1974). Spheroid chromatin units (v bodies). *Science* **183**: 330–332.
- Osbourn, A.E., and Field, B.** (2009). Operons. *Cell. Mol. Life Sci.* **66**: 3755–3775.
- Oudet, P., Gross-Bellard, M., and Chambon, P.** (1975). Electron microscopic and biochemical evidence that chromatin structure is a repeating unit. *Cell* **4**: 281–300.
- Papadopoulou, K., Melton, R.E., Leggett, M., Daniels, M.J., and Osbourn, A.E.** (1999). Compromised disease resistance in saponin-deficient plants. *Proc. Natl. Acad. Sci. USA* **96**: 12923–12928.
- Qi, X., Bakht, S., Leggett, M., Maxwell, C., Melton, R., and Osbourn, A.** (2004). A gene cluster for secondary metabolism in oat: Implications for the evolution of metabolic diversity in plants. *Proc. Natl. Acad. Sci. USA* **101**: 8233–8238.
- Qi, X., Bakht, S., Qin, B., Leggett, M., Hemmings, A., Mellon, F., Eagles, J., Werck-Reichhart, D., Schaller, H., Lesot, A., Melton, R., and Osbourn, A.** (2006). A different function for a member of an ancient and highly conserved cytochrome P450 family: From essential sterols to plant defense. *Proc. Natl. Acad. Sci. USA* **103**: 18848–18853.
- Robinson, P.J., Fairall, L., Huynh, V.A., and Rhodes, D.** (2006). EM measurements define the dimensions of the “30-nm” chromatin fiber: Evidence for a compact, interdigitated structure. *Proc. Natl. Acad. Sci. USA* **103**: 6506–6511.
- Shimura, K., et al.** (2007). Identification of a biosynthetic gene cluster in rice for momilactones. *J. Biol. Chem.* **282**: 34013–34018.
- Sproul, D., Gilbert, N., and Bickmore, W.A.** (2005). The role of chromatin structure in regulating the expression of clustered genes. *Nat. Rev. Genet.* **6**: 775–781.
- Swaminathan, S., Morrone, D., Wang, Q., Fulton, B.D., Peters, R.J.** (2009). CYP76M7 is an *ent*-cassadiene C11 α -hydroxylase defining a second multifunctional diterpenoid biosynthetic gene cluster in rice. *Plant Cell* **21**: 3315–3325.doi/.
- Tsukamoto, T., Hashiguchi, N., Janicki, S.M., Tumber, T., Belmont, A.S., and Spector, D.L.** (2000). Visualization of gene activity in living cells. *Nat. Cell Biol.* **2**: 871–878.
- Tumber, T., Sudlow, G., and Belmont, A.S.** (1999). Large-scale chromatin unfolding and remodeling induced by VP16 acidic activation domain. *J. Cell Biol.* **145**: 1341–1354.
- Volpi, E.V., Chevret, E., Jones, T., Vatcheva, R., Williamson, J., Beck, S., Campbell, R.D., Goldsworthy, M., Powis, S.H., Ragoussis, J., Trowsdale, J., and Sheer, D.** (2000). Large-scale chromatin organization of the major histocompatibility complex and other regions of

- human chromosome 6 and its response to interferon in interphase nuclei. *J. Cell Sci.* **113**: 1565–1576.
- Washida, H., Sugino, A., Messing, J., Esen, A., and Okita, T.W.** (2004). Asymmetric localization of seed storage protein RNAs to distinct subdomains of the endoplasmic reticulum in developing maize endosperm cells. *Plant Cell Physiol.* **45**: 1830–1837.
- Watson, J.D., and Crick, F.H.C.** (1953). The structure of DNA. *Cold Spring Harb. Symp. Quant. Biol.* **18**: 123–131.
- Wegel, E., Vallejos, R.H., Christou, P., Stoger, E., and Shaw, P.** (2005). Large-scale chromatin decondensation induced in a developmentally activated transgene locus. *J. Cell Sci.* **118**: 1021–1031.
- Wilderman, P.R., Xu, M., Jin, Y., Coates, R.M., and Peters, R.J.** (2004). Identification of syn-pimara-7,15-diene synthase reveals functional clustering of terpene synthases involved in rice phytoalexin/allelochemical biosynthesis. *Plant Physiol.* **135**: 2098–2105.
- Williams, R.R., Broad, S., Sheer, D., and Ragoussis, J.** (2002). Subchromosomal positioning of the epidermal differentiation complex (EDC) in keratinocyte and lymphoblast interphase nuclei. *Exp. Cell Res.* **272**: 163–175.
- Wong, S., and Wolfe, K.H.** (2005). Birth of a metabolic gene cluster in yeast by adaptive gene relocation. *Nat. Genet.* **37**: 777–782.
- Woodcock, C.L., and Dimitrov, S.** (2001). Higher-order structure of chromatin and chromosomes. *Curr. Opin. Genet. Dev.* **11**: 130–135.